

# Multiple Tipping Points and Optimal Repairing in Interacting Networks

Antonio Majdandzic,<sup>1</sup> Lidia A. Braunstein,<sup>1,2</sup> Chester Curme,<sup>1</sup> Irena Vodenska,<sup>1,3,4</sup> Sary Levy-Carciente,<sup>1,5</sup> H. Eugene Stanley,<sup>1</sup> and Shlomo Havlin<sup>1,6</sup>

<sup>1</sup>*Center for Polymer Studies and Department of Physics,  
Boston University, Boston, MA 02215, USA*

<sup>2</sup>*Departamento de Física, Facultad de Ciencias Exactas y Naturales,  
Universidad Nacional de Mar del Plata,  
Funes 3350, 7600 Mar del Plata, Argentina*

<sup>3</sup>*Administrative Sciences Department, Metropolitan College,  
Boston University, Boston, Massachusetts 02215 USA*

<sup>4</sup>*Center for finance, law and policy,  
Boston University, Boston, Massachusetts 02215 USA.*

<sup>5</sup>*Economics and Social Sciences Faculty,  
Central University of Venezuela, Caracas, Venezuela*

<sup>6</sup> *Department of Physics, Bar-Ilan University, 52900 Ramat-Gan, Israel*

(Dated: Version February 1, 2015.)

## Abstract

Systems that comprise many interacting dynamical networks, such as the human body with its biological networks or the global economic network consisting of regional clusters, often exhibit complicated collective dynamics. To understand the collective behavior of these systems, we investigate a model of interacting networks exhibiting the fundamental processes of failure, damage spread, and recovery. We find a very rich phase diagram that becomes exponentially more complex as the number of networks is increased. In the simplest example of  $n = 2$  interacting networks we find two critical points, 4 triple points, 10 allowed transitions, and two “forbidden” transitions, as well as a manifold of metastable regions represented by complex hysteresis. Knowing and understanding the phase diagram have an immediate practical implication; it enables us to find the optimal strategy for repairing partially or fully damaged interconnected networks. To support our model, we analyze an example of real interacting financial networks and find evidence of rapid dynamical transitions between well-defined states, in agreement with the predictions of our model.

PACS numbers:

Most real networks are not isolated structures but interact with other network structures. As a result, much research has been focused on the dynamics of interdependent [1–7] and multilayer [8, 9] networks. Recent studies on network repair [10–12] have shown the importance of recovery of nodes as a process which leads to reverse transitions, hysteresis effects, and such phenomena as spontaneous recovery [10, 13].

The cardiovascular and nervous systems in the human body are examples of two dynamically interacting physiological networks [14, 15]. Diseases often result from complex pathological conditions that involve a dynamical interaction [16–18] with positive or negative feedback between different functional subsystems in the body. Similarly, in the global economy there is a hierarchy of clustered and more tightly connected countries, often grouped geographically, that are further interconnected to one large global interacting economic and financial network [19–21]. To understand the behavior of these systems using network science, we develop a model of interacting networks with nodes that can recover from failure and we examine the resulting phase diagram. The phase diagram we find is very rich, and the number of tipping points grows either linearly (critical points) or exponentially (triple points, transition lines) as the number of interacting networks in the system is increased. We present our method and the results in detail for the simplest case of  $n = 2$  interacting networks, which can be easily generalized to any number of interacting networks.

Our model of a generic system consisting of interacting dynamical networks captures the important events found in real-world interacting networks, i.e., node failure [22, 23], systemic damage propagation [24], and node recovery [10, 13, 26]. In our model we first describe the structure of the system and then describe the rules governing the dynamic behavior of the processes occurring within the system.

The structure of our system for the  $n = 2$  case is modeled as follows. We start with two isolated networks, network A and network B, and for simplicity we assume that both networks have the same number of nodes  $N$  and the same degree distribution  $f(k)$  (these assumptions can be relaxed with a cost of additional complication, but the results are qualitatively similar). We assume that within each network the nodes are randomly connected. Now, to allow networks A and B to interact, we introduce interdependency links that connect nodes across the two networks [2]. This can be achieved in different ways, and we use a simple one-to-one dependency: each node in network A is connected to exactly one node in network B, and vice versa. The pairs of nodes of both networks are chosen randomly.

The dynamic behavior of our system is governed by two categories of event—failure and recovery—and we assume that every node is in either a failed or an active state. Node failure can result from internal failure or from the spread of damage from neighbor nodes in either the same network or the interdependent network. We thus assume that there are three ways a node can fail: (i) internally induced failure, when a node’s internal integrity has been compromised, e.g., an organ in the body can fail due to a malfunction within the organ or a company can fail due to bad management, (ii) externally induced failure through failure propagation due to connections with failed nodes within the node’s own network, and (iii) failure induced through the dependency link as a result of being dependent on a failed node from another (opposite) network. Apart of these three types of failures, we assume the existence of associated simple recovery processes for every type of failure. We specify quantitatively each of these processes below.

- (i) **Internal failure (I)**. We assume that in both networks any node can fail due to internal problems, independent of other nodes. For each node in network A we assume that there is probability  $p_A dt$  that the node will fail internally during any time period  $dt$ . The equivalent parameter in Network B is  $p_B$ .
- (ii) **External failure (E)**. Every node in network A and network B is connected by links to nearby nodes in its own network. These nodes constitute the node’s neighborhood. The number of links a node has within the network indicates its *degree* or *connectivity*, denoted by  $k$ . If a large number of nodes in a node’s neighborhood have failed, i.e., if the neighborhood is substantially damaged, we assume that the probability that the node itself will fail is increased. As in Refs. [10] and [27], we use a threshold rule to define a *substantially damaged* neighborhood, which is a neighborhood containing  $\leq m$  active nodes, where  $m$  is a fixed integer threshold. If node  $j$  has  $> m$  active neighbors during time  $dt$ , we consider its neighborhood to be “healthy” and there is no risk of external failure. On the other hand, if  $j$  has  $\leq m$  active neighbors during time  $dt$ , there is a probability  $r_A dt$  (for network A) or  $r_B dt$  (for network B) that node  $j$  will externally fail. (For an explanation of why  $r_A$  and  $r_B$  are not set to 1 and why they are necessary, see Note 1 in Methods).
- (iii) **Dependency failure (D)**. In the case of two interdependent networks (A and B) we assume that each node in the first network is dependent on a node in the second

network via an interdependent link, and vice versa. We assume that if one node in the pair fails there is a finite (but not 100%) probability,  $r_d dt$ , that during time  $dt$  the other node in the pair will fail as well. This indicates the probability that the damage will spread through the interdependency link.

(iv) **Recovery.** We assume that there is a reversal process, a recovery from each of these three types of failure. A node recovers from an *internal* failure after a time period  $\tau \neq 0$ , it recovers from an *external* failure after time  $\tau'$ , and from a *dependency* failure after time  $\tau''$ . In simulations, and without loss of generality, we use  $\tau = 100$ , and for simplicity we set  $\tau' = \tau'' = 1$  to take into account the assumption that real-world systems usually require a longer time period to recover from internal problems (physical faults) then from a lack of environmental support. Changing the numerical values however, does not introduce any qualitative difference.

(iv) **Activity notation.** Every node is in one of two states: active or failed. A node is considered active in the observed moment, if it is not experiencing internal (I), external (E), or dependency (D) failure.

## I. RESULTS

### A. Mean field theory

We characterise this system by studying the order parameters chosen naturally as the fraction of active nodes in network A and network B,  $z_A$  and  $z_B$ , respectively. For purposes of calculation, however, we first concentrate on the complementary and equally intuitive fraction of *failed* nodes  $a_A$  and  $a_B$ , in networks A and B respectively ( $a_A = 1 - z_A$ ,  $a_B = 1 - z_B$ ).

Using the mean field theory presented in Methods, Note 2, we obtain two coupled equations that connect  $a_A$  and  $a_B$ , which the system must satisfy in the equilibrium

$$a_A = p_A^* + r_d a_B (1 - p_A^*) + \sum_k f(k) F(k, a_A) [r_A - p_A^* r_A - r_A r_d a_B + p_A^* r_A r_d a_B] \quad (1)$$

$$a_B = p_B^* + r_d a_A (1 - p_B^*) + \sum_k f(k) F(k, a_B) [r_B - p_B^* r_B - r_B r_d a_A + p_B^* r_B r_d a_A] \quad (2)$$

Here  $F(k, x) = \sum_{j=0}^m \binom{k}{j} x^{k-j} (1-x)^j$ , and we have also introduced simplifying parameters  $p_A^* \equiv e^{-p_A \tau}$  and  $p_B^* \equiv e^{-p_B \tau}$  to make the equation more elegant and to reduce the number of parameters by replacing  $p_A$ ,  $p_B$ , and  $\tau$  that appear as a product. We find that the parameters  $p_A^*$  and  $p_B^*$  are very convenient to work with because they correspond to the fraction of internally failed nodes in network A and network B, respectively.

Despite the seeming complexity of Eqs. (1) and (2), note that there are only two unknown variables,  $a_A$  and  $a_B$ , and that all other parameters are fixed. These two equations define two curves in the  $(a_A, a_B)$  plane.

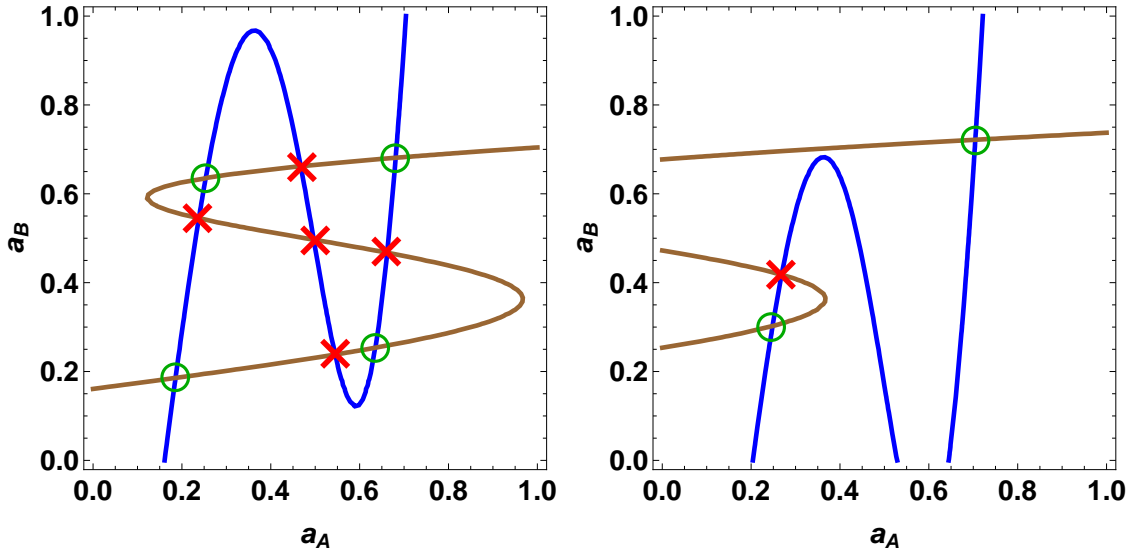


FIG. 1: **Graphical representations of the mean field equations for a system with two interdependent networks** ( $k = 16$ ,  $m = 8$ ). **a)** The blue and brown curve represent Eq. (2) and Eq. (3), respectively, for  $p_A^* = p_B^* = 0.16$ ,  $r_A = r_B = 0.60$  and  $r_d = 0.15$ . There are nine intersections, representing mathematical solutions for network activities  $a_A$  and  $a_B$ . Four of them are stable solutions (green circles) representing physical states that we also observe in our simulations, and five are unstable solutions (red crosses). **b)** Example for  $p_A^* = 0.20$ ,  $p_B^* = 0.24$ ,  $r_A = r_B = 0.60$  and  $r_d = 0.15$ . Here we obtain two stable and one unstable solution. The two stable solutions correspond to 11 state (both networks are at high activity) and 22 state (both networks are at low activity).

Figure 1a shows a graphical representation of the curves for a random regular [15, 28] network (in which all the nodes have the same degree) with degree of  $k = 16$  and threshold  $m = 8$ , for the symmetric parameter values  $p_A^* = p_B^* = 0.16$ ,  $r_A = r_B = 0.60$ , and  $r_d = 0.15$ .

The size of each network is  $N = 2 \times 10^4$ . The blue curve is a graphical representation of Eq. (1), and the brown curve is defined by Eq. (2). The curves, like two “ropes,” create a “knot” that can have up to nine intersections, representing mathematical solutions of the system of equations. Not all of these solutions represent observable physical states, however. Some of them turn out to be unstable and we need to discard them. To see that, observe one of the curves in Fig. 1a, for example the blue curve described by Eq. (2). We can think of this curve as describing the fraction of failed nodes  $a_A$  in network A as a function of  $a_B$  (the fraction of failed nodes in network B), keeping everything else fixed. If we increase damage done to network B (i.e. we increase  $a_B$ ) and keep everything else constant, some damage will undoubtedly spread to network A. Thus we expect that when  $a_B$  is increased,  $a_A$  must also increase (it would be very unusual if one network improves its activity as a result of damaging the other network, in our model where activities of the two networks are positively correlated). We conclude that the parts of the blue and brown curve that produce physical solutions are only those where  $a_A$  and  $a_B$  increase together or decrease together along the curve. This elimination leaves only four states in Fig. 1a that are stable (green circles), while the other five states are unstable (red crosses), for this particular choice of parameters. Generally, for any choice of parameters, we have between one and four physical states. Figure 1b shows the scenario for the same network system when  $p_A^* = 0.20$ ,  $p_B^* = 0.24$ ,  $r_A = r_B = 0.60$ , and  $r_d = 0.15$ . In this case we have two stable states and one unstable. This mean field theory calculation agrees well with the states that we observe in our simulation, as we will demonstrate later.

Note that our choice of  $r_d$  value is quite small. If  $r_d$  is too large, we find that the damage spreads through dependency links extremely efficiently and the only possible stable state is total system collapse. The extreme vulnerability of interdependent networks is well-known [2, 24]. Because there is always at least one functional stable state in biological or man-made systems, total system collapse as the only stable state is not realistic. Thus we need the  $r_d$  parameter to “soften” the dependency links and allow a more realistic behavior.

The four physical solutions found above correspond to the following four scenarios: (i) when there is high activity in both network A and network B (denoted “11” or “up-up”), (ii) when there is high activity in network A and low activity in network B (“12” or “up-down”), (iii) when there is low activity in network A and high activity in network B (“21” or “down-up”), and (iv) when there is low activity in both network A and network B (“22”

or “down-down”).

Depending on the parameters, we obtain between one and four stable states. Each of the states exists in a certain volume of the multi-dimensional space of parameters. Results of the mean field theory calculation for a particular set of parameters are presented in Fig. 2a-d as a phase diagram with four layers. Figure 2 shows the regions in which each of the four states exist in the  $(p_A^*, p_B^*)$  parametric sub-space, when other parameters are fixed at values  $r_A = r_B = 0.60$  and  $r_d = 0.15$ , with  $k$  and  $m$  remaining the same as before.

For example, in Fig. 2a the green area indicates the region where the 11 state exists. This state (phase) is bounded with a smooth boundary of three colors. If the boundary is crossed (by increasing  $p_A^*$  and  $p_B^*$ ), the system makes a transition to either state 12 (if the orange line is crossed), state 22 (if the blue line is crossed), or state 21 (if the purple line is crossed). The arrows indicate transitions. In Fig. 2a there are two triple points (black points) that mark the change in the transition type and where three different states can exist. The blue area in Fig. 2b indicates the 22 state. This layer of the phase diagram has two triple points as well, and three possible transitions ( $22 \rightarrow 12$ ,  $22 \rightarrow 11$ , and  $22 \rightarrow 21$ ).

Figures 2c and 2d show the regions of state 21 (purple) and state 12 (orange), respectively. Each has two different transitions and one critical [25] point. For example, there are two possible ways out of state 21 (Fig. 2c): by a transition to the 11 (green arrow) state or the 22 (blue arrow) state. Note that the different state regions (Figs. 2a, 2b, 2c, and 2d) are not disjoint sets but there is an overlap, resulting in 2-fold, 3-fold, or even 4-fold hysteresis regions.

The state in which the system is found depends on the initial conditions or the system’s past. There are a total of 10 different transitions ( $11 \rightarrow 12$ ,  $11 \rightarrow 22$ ,  $11 \rightarrow 21$ ,  $12 \rightarrow 11$ ,  $12 \rightarrow 22$ ,  $21 \rightarrow 11$ ,  $21 \rightarrow 22$ ,  $22 \rightarrow 12$ ,  $22 \rightarrow 21$  and  $22 \rightarrow 11$ ) that connect different layers of the phase diagram (states 11, 12, 21, and 22), much like elevators connecting different floors. Transitions  $12 \rightarrow 21$  and  $21 \rightarrow 12$  are the only missing (“forbidden”) combinations. Although regions 12 and 21 do overlap, there is no a direct transition connecting these two states. These transitions would correspond to the unusual combination in which one network recovers (transitions to a higher activity) and simultaneously the other network fails. Thus a transition from state 12 to state 21 requires the use of an intermediate state (11 or 22). A more detailed discussion of the absence of these two transitions can be found in Methods, part 3. The set of all allowed and forbidden transitions is presented in Fig. 2e. The total



phase diagram (all four layers on top of each other) is presented in Fig. 3. Here, color lines represent the boundaries of four states, with each color corresponding to the boundary of one state, e.g., the green line is a boundary of the 11 state. Note that there is a small central “window” where all four states are possible.

We next can examine the activity profile for various cross-sections in the phase diagram. In Figure 3 we choose two representative cross sections (dashed straight lines) to measure activity  $z_A = 1 - a_A$  as  $p_A^*$  and  $p_B^*$  change. The black dashed line is defined by the equation  $p_B^* = 0.1 + 4/3p_A^*$  and the red dashed line by  $p_B^* = 0.4 - p_A^*$ . Figure 4a shows the activity measured in simulations of network A as we move along the black dashed line, changing both  $p_A^*$  and  $p_B^*$  and preserving the relation  $p_B^* = 0.1 + 4/3p_A^*$ . We perform simulations for various initial conditions and find (Fig. 4a) three different states denoted by green, orange and blue colors, which we identify as 11, 12, and 22 states. We find four different transitions:  $11 \rightarrow 12$ ,  $12 \rightarrow 22$ ,  $12 \rightarrow 11$ , and  $22 \rightarrow 12$ . The solid lines show the mean field theory (MFT) prediction [Eqs. (1) and (2)] for the activity of network A. The good agreement shows that the mean field theory correctly captures all the properties of the system. We note that qualitative agreement between the MFT and the simulations is better for higher values of  $k$ , because for higher  $k$  the fluctuations are smaller, which improves the accuracy of the MFT. Figure 4b shows the activity when moving along the red dashed line. Here we obtain four states and six different transitions.

The phase diagram of a system of  $n = 2$  interacting networks is much richer than the phase diagram of a single network with damage and recovery [10]. The analytical results we presented here for  $n = 2$  can be generalized to  $n$  interacting networks in any topological configuration, although as  $n$  increases they become increasingly difficult to visualize. In general, a system with  $n$  interacting networks can have up to  $2^n$  physical states. The maximum number of critical points grows linearly with  $n$  while the upper limit for the number of triple points grows exponentially.

## B. The problem of optimal repairing

Knowing and understanding the phase diagram of interacting networks enable us to answer some fundamental and practical questions. A partially or completely collapsed system of  $n \geq 2$  interacting networks in which some of them are in the low activity state is a

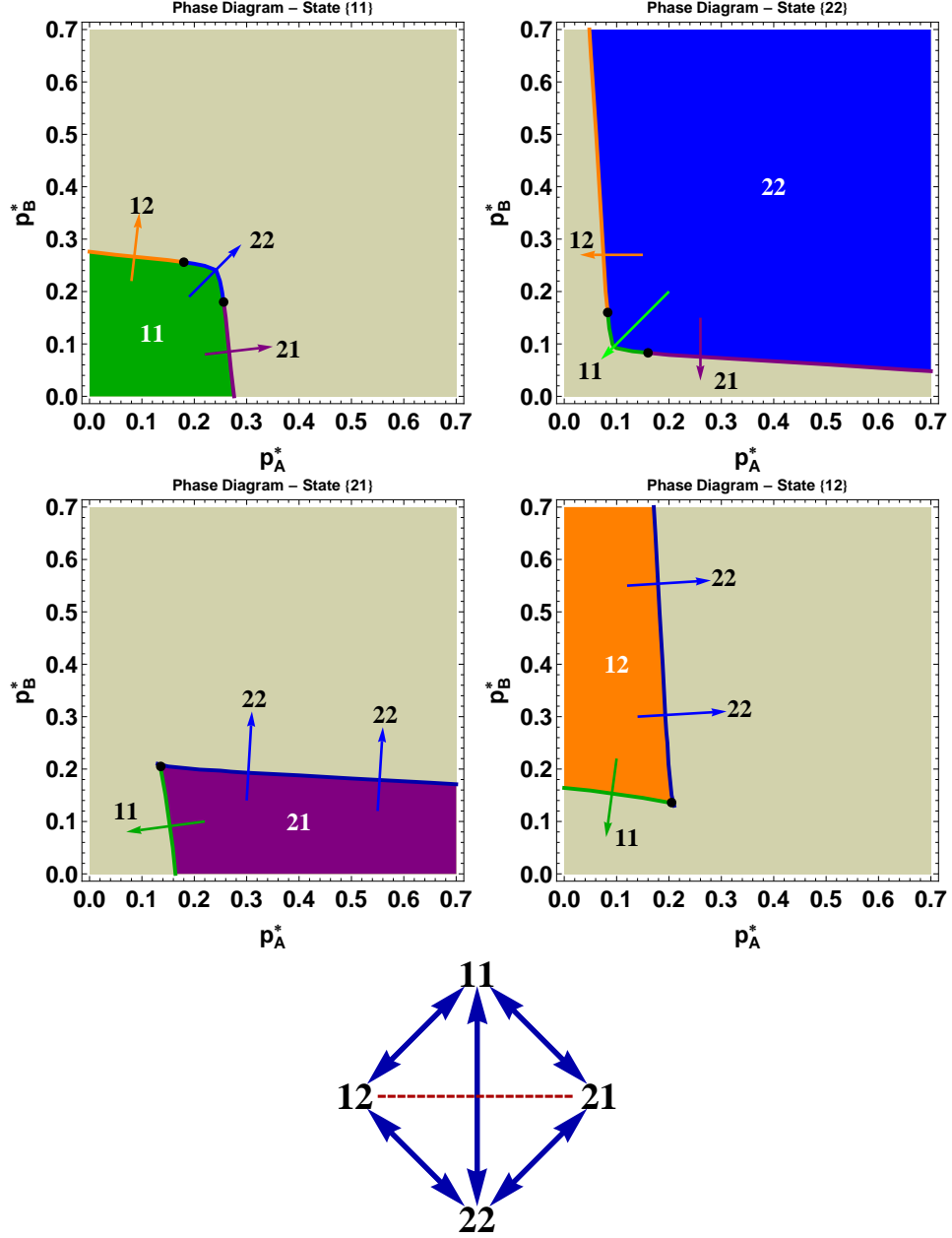


FIG. 2: Four layers of the phase diagram and the transitions connecting them. a) Region of 11 state, in green. Possible transitions are 11  $\rightarrow$  12 (orange line), 11  $\rightarrow$  22 (blue line) and 11  $\rightarrow$  21 (purple line). This layer of the phase diagram has two triple points, marked as black points. b) Region of 22 state (blue), with two triple points and three transitions. c) Region of 21 state (purple), with two transition lines (to 11 and 22 state) that merge in a critical point. d) Region of 12 state (orange), with two transition lines (to 11 and 22 state) that merge in a critical point. e) Illustration showing states (11, 12, 21 and 22) with allowed (blue arrows) and "forbidden" (dashed red line) transitions.

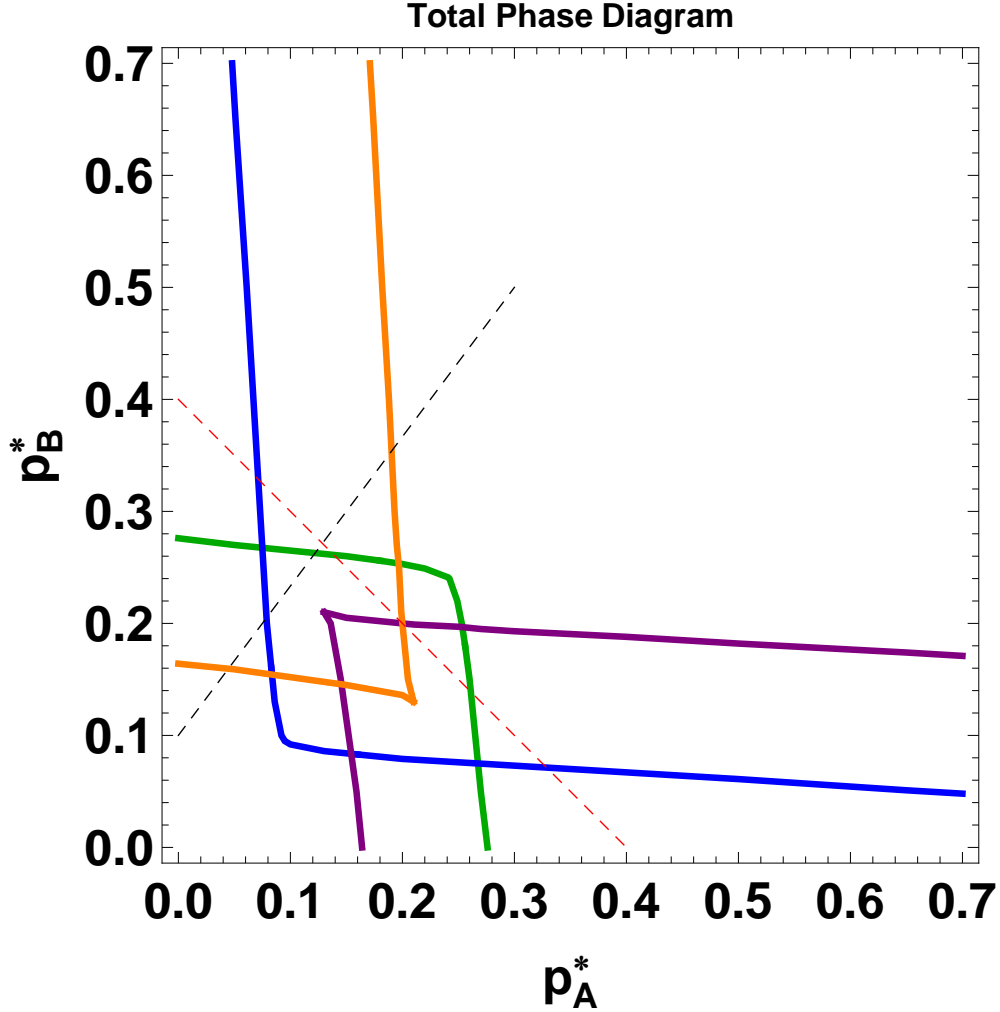


FIG. 3: **Total phase diagram, with all four layers.** Solid lines represent the border of region 11 (green), 22 (blue), 12 (orange) and 21 (purple). Dashed lines represent cross-sections where we calculate the activity profile, shown in Figure 4.

scenario common in medicine, e.g., when diseases or traumas affect the human body and a few organs are simultaneously damaged and need to be treated, and the interaction between the organs is critical. It is also common in economics, when two or more coupled sectors of the economy [20] experience simultaneous problems, or when a few geographical clusters of countries experience economic difficulties. The practical question that arises is: What is the most efficient strategy to repair such a system? Many approaches are possible if resources are unlimited, but this is usually not the case and we would like to minimize the resources that we spend in the repairing process.

For simplicity, consider two interacting networks, both damaged (low activity). Is re-

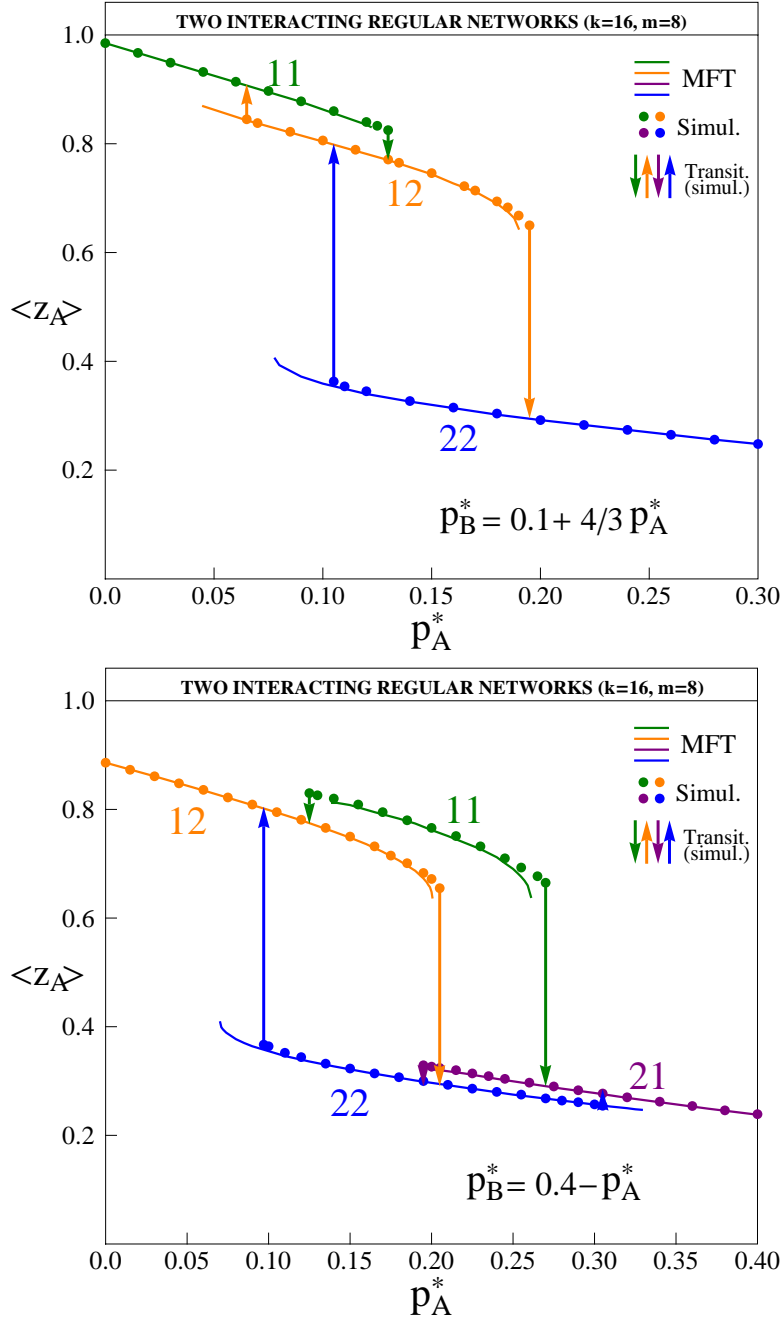


FIG. 4: **States, transitions and hysteresis loops for two activity profiles.** a) Activity  $z_A$  of network A, as measured in simulations (dots) and predicted by mean field theory (solid lines), along the cross section defined by the black dashed line in Fig 3. Parameters  $p_A^*$  and  $p_B^*$  are changed, preserving the relation  $p_B^* = 0.1 + 4/3 p_A^*$ . Transitions are denoted by arrows. b) Same for the cross section defined by  $p_B^* = 0.4 - p_A^*$  (red dashed line in Fig. 3). Here we obtain 4 states and 6 different transitions, giving rise to more complex hysteresis loops.

pairing both networks simultaneously the more efficient approach, or repairing them one after the other? What is the minimum amount of repair needed to make the system fully functional again? In other words, what is the minimum number of nodes we need to repair in order to bring the system to the functional 11 (“up-up”) state, and how do we allocate repairs between the two networks? An optimal repairing strategy is essential when resources needed for repairing are limited or very expensive, when the time to repair the system is limited, or when the damage is still progressing through the system, threatening further collapse, and a quick and efficient intervention is needed.

We show below that this problem is equivalent to finding the minimum Manhattan distance between the point in the phase diagram where the damaged system is currently situated, and the recovery transition lines to the 11 region. The Manhattan distance between two points is defined as the sum of absolute horizontal and vertical components of the vector connecting the points, with defined vertical and horizontal directions. It is a driving distance between two points in a rectangular grid of streets and avenues. In our phase diagram, it is equal to  $|\Delta p_A^*| + |\Delta p_B^*|$ . It turns out that two triple points of the phase diagram play a very important role in this fundamental problem. We find that these special points have a direct practical meaning and are not just a topological or thermodynamic curiosity.

To show this, we start by making some simplifying but reasonable assumptions. First, we assume that only internal failures can be repaired by human hands, since these failures are physical faults in nodes (any external and dependency failures and recoveries are “environmental,” and are a spontaneous recognition of the changing neighborhood of a node). We mentioned above that the parameters  $p_A^*$  and  $p_B^*$  correspond to fractions of internally failed nodes in networks A and B, respectively. This implies that the number of internally failed nodes repaired in, say, network A, is directly proportional to the change of  $p_A^*$ . Hence repairing nodes in networks A and B means decreasing  $p_A^*$  or  $p_B^*$ . We also assume that these repairs are done quickly enough that there is only a small probability that the newly repaired nodes will internally fail again before the repair process is completed. The total number of repaired nodes is therefore  $N_{\text{rep}} = N(|\Delta p_A^*| + |\Delta p_B^*|)$ , and it is proportional to the Manhattan distance between the starting and final point in the phase diagram.

To optimize repairing we need to minimize this metric. Figure 5 shows the solution to the minimization problem, and a detailed discussion is provided in Methods. The different colors in Fig. 5 correspond to the different optimal repair strategies, which depend on the

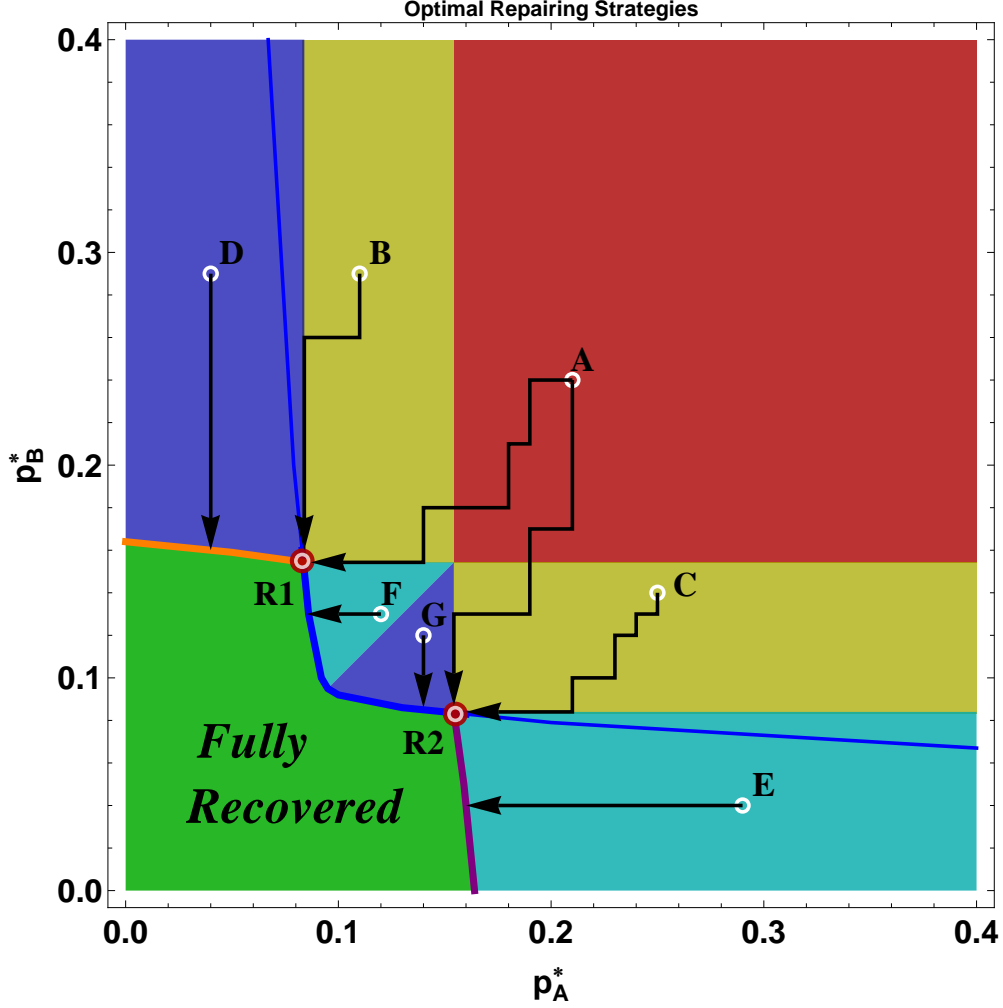


FIG. 5: **Optimal repairing strategies.** The solution to the problem of least expensive repairing corresponds to finding the minimal Manhattan distance from the point where the collapsed system is initially situated, and the border of the green region. In the red square sector (point A for example), there are two solutions and it is equally optimal to reach any of the two triple points R1 and R2 by decreasing  $p_A^*$  and  $p_B^*$ . In the yellow regions, it is optimal to reach only one triple point - R1 for the sector containing point B, or R2 for the sector containing point C. In the dark blue regions it is optimal to decrease  $p_B^*$  only, and in the light blue regions it is optimal to decrease  $p_A^*$  only. Note that triple points represent the solution of the optimal repairing for the warm color regions (red and yellow).

failure state of the system. If the system is initially at point A, both networks are in a low activity state, i.e., they are non-functional. Our goal is to decrease  $p_A^*$  and  $p_B^*$  and arrive to the region where the system is fully recovered (the green region) by performing a

minimal number of repairs, i.e. minimal  $N_{\text{rep}}$ . We find that for any point in the red region there are actually two closest points in the green region, at an equal Manhattan distance away from the red region point. These two points are the triple points R1 and R2 shown in Fig. 5. Although R1 may be closer to point A than R2 by Euclidian distance, the Manhattan distance is the same. Thus two equally good repairing strategies are available. One involves allocating more node repairs to network A, and the other allocating more repairs to network B. For the yellow regions (points B and C), the closest points by Manhattan distance are R1 (for point B) or R2 (for point C). Here only one triple point represents the optimal solution. Note that the path samples in Fig. 5 are “zig-zag” in shape (to highlight that we are minimizing  $|\Delta p_A^*| + |\Delta p_B^*|$ ), but even when a diagonal path (direct straight line) to a triple point is used, the Manhattan distance is the same. For the dark blue regions (points D and G), the optimal strategy is to decrease  $p_B^*$  only, until the system is recovered. Similarly, for the light blue regions (points E and F), the optimal strategy is to decrease only  $p_A^*$ .

From our optimal repairing strategy analysis we find that the order of repair (the specific path taken between the initial point and final point) does not affect the final result. Minimizing the Manhattan distance only determines the optimal destination point. Therefore, there is actually a set of paths corresponding to equally optimal repairing processes.

### C. States and transitions in Real World Networks

In relatively small networks ( $N \approx 10\text{--}1000$ ) fluctuations are very large. Thus, in small network systems exhibiting multistability it is possible to observe phase flipping [10, 13, 29] between different states. Figure 6a shows the fraction of active nodes for both networks, in time, for a symmetric choice of parameters,  $p_A^* = p_B^* = 0.21$ ,  $r_A = r_B = 0.60$ , and  $r_d = 0.15$ , when each network has only  $N = 100$  nodes. Large fluctuations cause the system to jump between the different states allowed for this set of parameters. Note that interdependent links cause the two networks to have partially dependent and correlated dynamics. Very often a transition in one network triggers a transition in the other. In Figure 6a we can identify examples of all four global states: 22, 11, 21 and 12. For example, at time  $t \approx 400$  both networks are in the high activity state (11), while at  $t \approx 620$  network A is in the low activity and network B in the high activity state (21). Because the controlled experimental changing of such parameters as  $p_A^*$  or  $p_B^*$  is usually impossible or hardly accessible in real-

world networks, we can exploit the phenomenon of phase flipping, use it as a probe to explore different layers of the phase diagram, and verify the existence of well-defined states and the transitions between them in a real-world network system. By observing the dynamics in a selected real-world interacting network, we find evidence of rapid transitions between different states (Fig. 6b) that strongly resemble the spontaneous phase switching seen in our model (Fig. 6a).

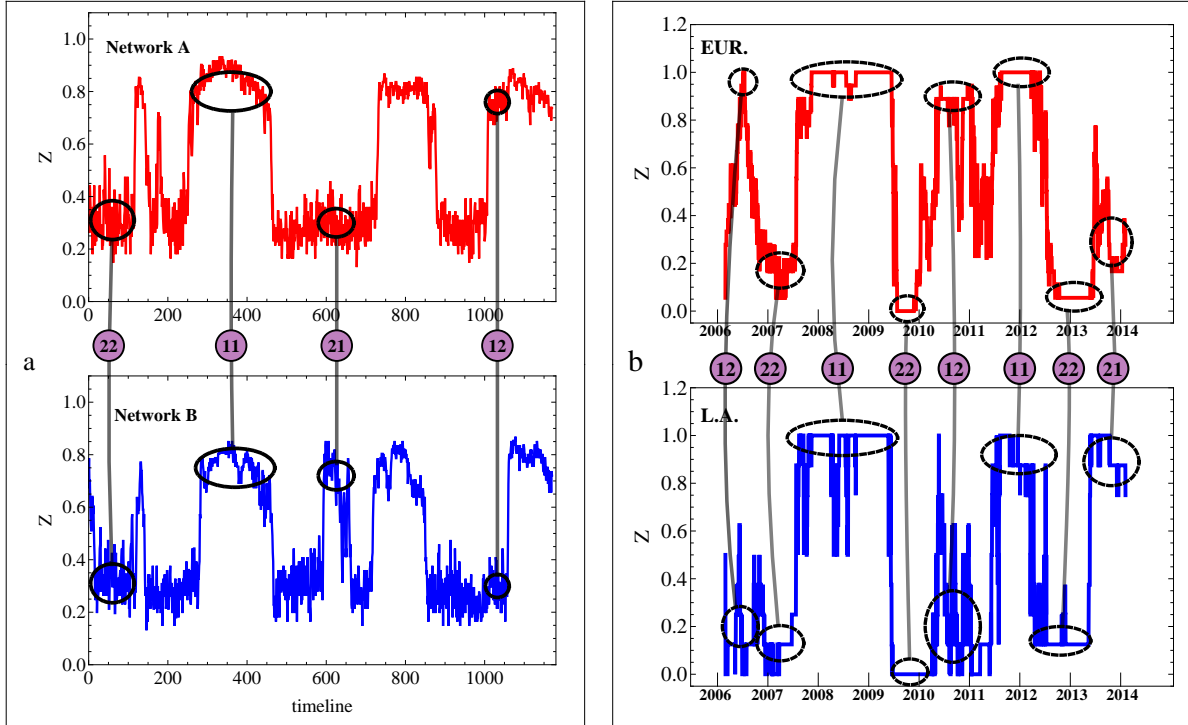


FIG. 6: **Collective states in simulated and real interacting networks.** **a** Simulation of the networks' dynamics, activity versus time, for  $N = 100$  and failure parameters  $p_A^* = p_B^* = 0.21$ ,  $r_A = r_B = 0.60$ ,  $r_d = 0.15$ , shows the switching of the system between different states. We can easily identify four collective states - 11, 22, 11, and 21. **b** Dynamics of two CDS geographical networks consisting of 18 European and 8 Latin American countries, shows very similar elements of the behavior: individual networks switching between well defined high activity and low activity states, as well as the correlated collective behavior of the two networks in interaction. We identify collective states 11, 22, 12 and 21 and mark them with connected black ovals. Note that since the CDS value grows with risk, a higher activity in a CDS network corresponds to bad economic news.

To test our model with a real-world example we analyze the sovereign debt 5-year credit



default swaps (CDSs) of 26 different countries from two geographical regions, Europe and Latin America. The full list of the countries given in Methods, Part 5 represents all European and Latin American countries that began to issue the CDS as early as 2005. A CDS is a derivative contract that protects against the default risk of an underlying reference asset as a result of a specific credit event, a kind of insurance against credit default. In a CDS the buyer pays the seller a premium for the recovery of a credit loss in case of default. The higher the risk of default, the higher the premium, so the value of a governmental CDS reflects the size and probability of a potential loss for an investor in governmental bonds of a particular country. A more detailed explanation of CDSs from an economic and financial perspective is given in Methods, Part 5. CDSs are leveraged instruments (small changes in the underlying variables on which the instrument is dependent can cause enormous changes in the value of the instrument) and their values are very sensitive to both negative and positive economic and political news emerging from various countries - they reflect the sentiment or investor's perception of risk and fear about a particular country's economy. When one country is experiencing problems, this fear might affect the CDS values in other countries, usually in the countries of the same geographical region first, and then in other countries. This behavior suggests that we can treat countries as nodes and geographical regions (e.g., Europe and South America) as interacting networks.

We examine the upward and downward movements of the CDS values in the 26 countries during the period June 2005–February 2014. We represent each country with one node that can have two states: active or failed. Since the CDS data is continuous, and in our model we have binary node states, we perform the following mapping to produce a binary state for each country. For each time  $t$ , we consider the interval  $[t - 252, t]$  of 252 business days (this number is usually taken as the number of business days in a year). If the CDS of a country has a net increase during that period, we consider the node of the country to be active at  $t$ . If it does not, it is inactive. Figure 6b shows the interaction of the two geographical CDS networks: Latin America and Europe. First we note that the networks indeed spend most of their time having either a very high activity or a very low activity (i.e., there are two well-defined single-networks states). We also observe that because of interactions between the two networks they can share transition moments between high and low activity, but sometimes these transitions occur independently. This behavior is very similar to the model behavior observed in Fig. 6a. We conclude that our network model successfully captures

the behavior of this real network, and it represents a plausible model to explain the most important elements of its behavior.

## II. METHODS

**1. Damage conductivity parameters.** Parameters  $r_A$  and  $r_B$  are introduced because they describe how easily the damage is conducted through the network. When  $r = 0$  there is no damage spread between the nodes, and when  $r = 1$  there is perfect damage conduction. Assuming that external failures occur with certainty would mean fixing  $r$  to be equal to 1. In the case of a single network with recovery it has been shown [10] that many important phenomena (e.g., spontaneous recovery) are lost when  $r = 1$ . The most interesting parts of the phase diagram are in fact where  $r$  is far from 1.

**2. Mean field theory.** Fractions  $a_A$  and  $a_B$  denote the fraction of nodes that are failed due to any of the three types of failures: internal (I), external (E), or dependency failure (D). We denote the probabilities that a node at a time of observation experiences a failure of I, E, or D type as  $P(I)$ ,  $P(E)$ , and  $P(D)$ , respectively. As a first approximation, we assume that these failures are mutually independent events. Considering network A first, we write an expression for the probability  $a_{A,k}$  that a node of degree  $k$  in network A has failed. The node can fail due to I, E, or D events or to a combination of them. Using the inclusion-exclusion principle for independent events, we write

$$a_{A,k} = P(I) + P(E) + P(D) - P(I)P(E) - P(I)P(D) - P(E)P(D) + P(I)P(E)P(D). \quad (3)$$

Next, we separately calculate  $P(I)$ ,  $P(E)$ , and  $P(D)$ .

**Calculating P(I)**, the probability that a randomly chosen node is internally failed at the time of observation.  $P(I)$  is also the average fraction of internally-failed nodes in a network, since internal failures are independent events. This is a Poisson process on individual nodes [10, 30], and therefore  $P(I) = e^{-p_A\tau}$ . Since parameters  $p_A$  and  $\tau$  come in this expression as a product, we can replace them with a single parameter,  $p_A^* \equiv e^{-p_A\tau}$ , which is bounded and also has the property  $0 \leq p_A^* \leq 1$ , and so  $P(I) = p_A^*$  for network A.

**Calculating P(E)**, the probability that a randomly chosen node with degree  $k$  has externally failed. Focusing once again on network A, without a loss of generality, we let  $F(k)$  be the probability that a node of degree  $k$  in network A is located in a critically damaged

neighborhood (where fewer than  $m + 1$  nodes are active). By definition, the time-averaged fraction of failed nodes (for any reason) in network A is  $0 \leq a_A \leq 1$ . In a mean-field approximation, this is also the average probability that a randomly chosen node in that network has failed. Using combinatorics, we obtain  $F(k, a_A) = \sum_{j=0}^m \binom{k}{j} a_A^{k-j} (1 - a_A)^j$  [10]. The probability that a node of degree  $k$  in network A has externally failed is then  $P(E) = r_A F(k, a_A)$ . An analogous result is valid for network B.

**Calculating P(D)**, the probability that a node has failed due to the failure of its dependent counterpart node in the other network. For network A, this probability is equal to the product of parameter  $r_d$  and the probability that a counterpart node in B has failed:  $P(D) = r_d a_B$ . In network B by analogy this probability is equal to  $r_d a_A$ .

Writing Eq. (1) for both networks and inserting the results for P(I), P(E), and P(D) after summing over all  $k$  (and noting  $a_A = \sum_k f(k) a_{A,k}$  and  $a_B = \sum_k f(k) a_{B,k}$ ), we get a system of two coupled equations that describes the system of networks,

$$a_A = p_A^* + r_d a_B (1 - p_A^*) + \sum_k f(k) F(a_A) [r_A - p_A^* r_A - r_A r_d a_B + p_A^* r_A r_d a_B] \quad (4)$$

$$a_B = p_B^* + r_d a_A (1 - p_B^*) + \sum_k f(k) F(a_B) [r_B - p_B^* r_B - r_B r_d a_A + p_B^* r_B r_d a_A]. \quad (5)$$

**3. "Forbidden" transitions.** Transition lines for  $12 \rightarrow 21$  and  $21 \rightarrow 12$  do not appear in our phase diagram, and it is quite easy to understand why. Lets assume that the transition line for  $12 \rightarrow 21$  does exist. To obtain that transition, the idea would be to simultaneously increase  $p_A^*$  and decrease  $p_B^*$  (i.e., increase the damage in one part of the system, and decrease in another part). Suppose we are in phase 12 and infinitesimally close to the supposed transition line. Considering the local geometry of this line, we may be able to observe its angle with respect to the  $p_A^*$  axis. If a transition occurs when increasing  $p_A^*$  and decreasing  $p_B^*$ , the tangent on the supposed line would have an angle of  $\theta \in [0, \frac{\pi}{2}]$ . From here it follows that by increasing  $p_A^*$  only, while keeping  $p_B^*$  constant, we would also make a transition (cross the transition line). The only other possibility would be that we were moving *along* the transition line, but this is easy to disprove because it would imply that the transition does not depend on  $p_A^*$ . If increasing  $p_A^*$  only, causes a transition, the transition must end in state 22, not 21. This is because if we only increase  $p_A^*$ , we increase damage to both network A (directly) and network B (indirectly, through the interdependent links).

**4. Geometry of the Manhattan distance minimisation problem.** The optimal

strategies shown in different colors in Fig. 5 are derived from the geometrical reasoning shown in Fig. 7. Figure 7a shows a plot of a series of curves consisting of points at identical Manhattan distances from point A (equidistant curves). They produce a “diamond” shape, and the minimal Manhattan distance between point A and the green region translates into the task of “fitting” the diamond so that it just touches the green region and its center is at A. The diamond in Fig. 7a touches the green region at two points—triple points, which are the solution to the minimisation problem. Figure 7b shows the solution for point F in the light blue region. Here the solution suggests a different strategy—decreasing only  $p_A^*$ .

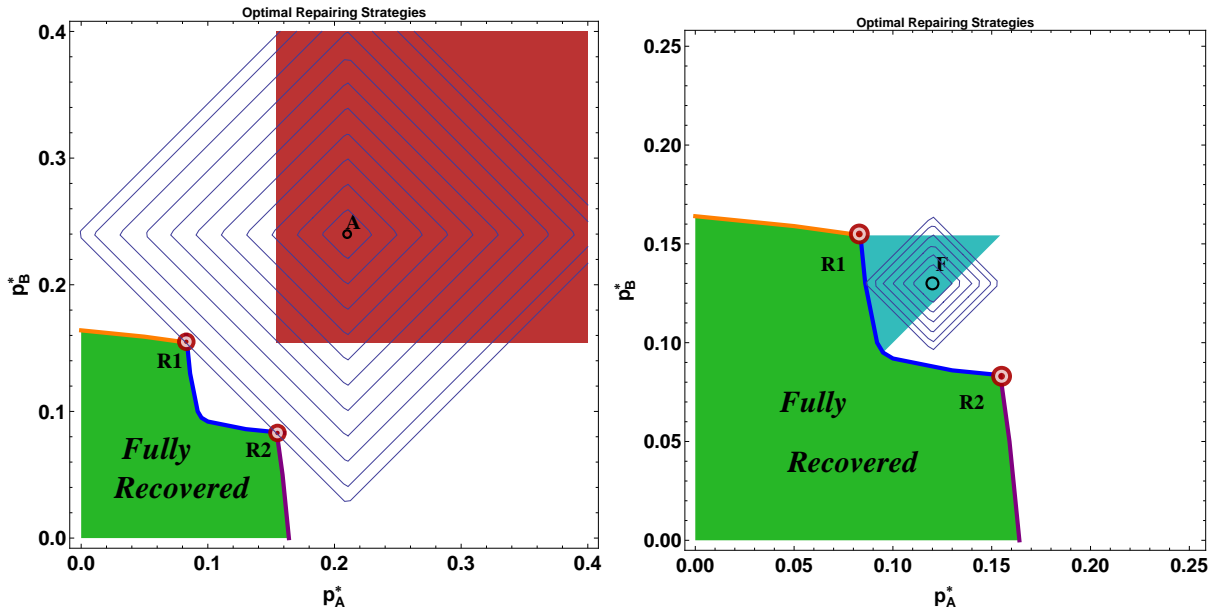


FIG. 7: **Minimum Manhattan distance problem.** **a** For the red sector, fitting the largest “diamond” barely touching the green region and having its center at point A, suggests there are two equally optimal solutions to the minimization problem. **a** The same geometrical construction for point F in the light blue region, suggests a unique solution: decreasing  $p_A^*$ .

**5. Credit default swaps.** Figure 6b shows an analysis of a set of European countries: France, Germany, Italy, Spain, Portugal, Belgium, Austria, Denmark, Sweden, Greece, Ukraine, Hungary, Poland, Croatia, Slovenia, Romania, Bulgaria, and Slovakia. All of these countries had a governmental CDS at 2005. The set of Latin American countries we analyzed consisted of Brazil, Colombia, Argentina, Mexico, Venezuela, Chile, Peru, and Panama. A CDS is typically used to transfer the credit exposure of fixed income products from one party to another. The buyer of the CDS is then obligated to make periodic payments to the

seller of the CDS until the swap contract matures. In return, the seller of the CDS agrees to compensate (pay off) the seller who holds this third party debt if this (third party) defaults on the issued debt.

A CDS is, in effect, an insurance against non-payment of a debt owed by a third party. The buyer of a CDS does not have to hold the debt of the third party but can speculate on the possibility that the third party will indeed default, and the buyer can purchase the CDS for this speculative purpose. CDSs were developed in the 1990s and, given their simple structure and flexible conditions, they are a major part of the credit derivative activity in the OTC market used to hedge credit risk. One of the most important aspects of a CDS is the definition of the “credit event” that triggers the CDS. These events include bankruptcy, obligation acceleration, obligation default, failure to pay, repudiation (moratorium), and restructuring. In the case of the sovereign bond market, the last three are typically included in the contracts. CDS premiums are used as a guide of risks appreciated by market participants, rather than being the measure of the strength of a particular economy. CDSs are used by portfolio investors to take advantage of short-term volatility, but as the last financial crisis demonstrated, CDSs are not able to anticipate long-term future risk, e.g., as in the case of sovereign bonds in which the underlying assets are 5y-10y bonds.

### **Acknowledgments**

We thank the DTRA, NSF (grants CMMI 1125290, CHE-1213217 and SES 1452061), Keck Foundation, European Commission FET Open Project (FOC 255987, FOC-INCO 297149) and Office of Naval Research for financial support. S.H. acknowledges the European EPIWORK, LINC and MULTIPLEX (EU-FET project 317532) projects, the Deutsche Forschungsgemeinschaft (DFG), the Israel Science Foundation, ONR and DTRA for financial support. L.A.B thanks UNMdP and FONCyT, PICT 0429/13 for financial support. S.L.C gratefully acknowledges the financial support of the Fulbright Program for visiting scholars. A.M. thanks Bijeli Zeko for useful discussions.

---

[1] G. D’Agostino, A. Scala (Eds.), *Networks of Networks: The Last Frontier of Complexity*. (Springer, 2014)

- [2] S. V. Buldyrev et al., *Nature* **464**, 1025 (2010).
- [3] J. Gao, S.V. Buldyrev, H.E. Stanley, S. Havlin. Networks formed from interdependent networks. *Nature Physics* **8**, 40-48 (2012).
- [4] Vespignani, Alessandro (2010). Complex networks: The fragility of interdependency. *Nature* **464** (7291): 984985.
- [5] Donges, J. F.; Schultz, H. C. H.; Marwan, N.; Zou, Y.; Kurths, J. (2011). Investigating the topology of interacting networks. *The European Physical Journal B* **84**
- [6] S.D.S. Reis et al., Avoiding catastrophic failure in correlated networks of networks. *Nature Physics* **10**, 762767 (2014).
- [7] A. Bashan et al., The extreme vulnerability of interdependent spatially embedded networks. *Nature Physics* **9**, 667672 (2013).
- [8] M. Kivel, A. Arenas, M. Barthelemy, J. P. Gleeson, Y. Moreno, M. A. Porter. Multilayer networks. *Journal of Complex Networks* **2** (3) 203-271 (2014).
- [9] G. Bianconi. Multilayer networks: Dangerous liaisons? *Nature Physics* **10**, 712714 (2014).
- [10] A. Majdandzic et al., Spontaneous recovery in dynamical networks. *Nature Physics*, **10**, 3438 (2014).
- [11] C. Liu et al., Modeling of self-healing against cascading overload failures in complex networks. *EPL* **107** 68003 (2014).
- [12] B. Podobnik, T. Lipic, D. Horvatic, A. Majdandzic, S. Bishop, H.E. Stanley. Predicting Lifetime of Dynamical Networks Experiencing Persistent Random Attacks. arXiv preprint, arXiv:1407.0952
- [13] B. Podobnik, A. Majdandzic, C. Curme, Z. Qiao, W.X. Zhou, H.E. Stanley, B. Li. Network risk and forecasting power in phase-flipping dynamical networks. *Physical Review E* **89**, 042807 (2014).
- [14] Newman, M. E. J. *Networks: An Introduction*. Oxford University Press, New York, (2010).
- [15] R. Cohen and S. Havlin, *Complex Networks: Structure, Robustness, and Function* (Cambridge University Press, Cambridge, 2010).
- [16] Vespignani, A. Modeling dynamical processes in complex socio-technical systems. *Nature Phys.* **8**, 3239 (2012).
- [17] Watts, D. J. & Strogatz, S. H. Collective dynamics of 'small-world' networks. *Nature* **393**, 440–442 (1998).

- [18] B. Buca and T. Prosen. Exactly Solvable Counting Statistics in Open Weakly Coupled Interacting Spin Systems. *Phys. Rev. Lett.* **112**, 067201 (2014).
- [19] G. Caldarelli, A. Chessa, F. Pammolli, A. Gabrielli & M. Puliga. Reconstructing a credit network. *Nature Physics* 9, 125126 (2013).
- [20] C. Curme et al., Emergence of statistically validated financial intraday lead-lag relationships. Preprint, arXiv:1401.0462.
- [21] X. Huang, I. Vodenska, S. Havlin, H.E. Stanley, Cascading failures in bi-partite graphs: model for systemic risk propagation. *Scientific reports* 3, 1219 (2013).
- [22] Albert, R., Jeong, H. & Barabasi, A. L. Error and attack tolerance of complex networks. *Nature* 406, 378382 (2000).
- [23] Schneider, C. M., Moreira, A. A., Andrade, J. S.Jr, Havlin, S. & Herrmann, H. J. Mitigation of malicious attacks on networks. *Proc. Natl Acad. Sci. USA* 108, 38383841 (2011)
- [24] R. Parshani et al., Epidemic Threshold for the Susceptible-Infectious-Susceptible Model on Random Networks. *Phys. Rev. Lett.* 104, 258701 (2010)
- [25] Dorogovtsev, S. N. & Goltsev, A. V. Critical phenomena in complex networks. *Rev. Mod. Phys.* 80, 12751335 (2008).
- [26] M. Stippingera, J. Kertszb, Enhancing resilience of interdependent networks by healing. *Physica A* 416, 481487 (2014).
- [27] Watts, D. J. A simple model of global cascades on random networks. *Proc. Natl Acad. Sci. USA* 99, 57665771 (2002).
- [28] Barabási, A. -L. & Albert, R. Emergence of scaling in random networks. *Science* **286**, 509–512 (1999).
- [29] T. A. Kesselring, G. Franzese, S.V. Buldyrev, H.J. Herrmann & H. E. Stanley. Nanoscale Dynamics of Phase Flipping in Water near its Hypothesized Liquid-Liquid Critical Point. *Scientific Reports* 2, 474 (2012).
- [30] T.L. Saaty, *Elements of queueing theory: with applications.* (McGraw-Hill, 1961)